



Anisotropic transport behavior of orbital-ordered $\text{Nd}_{0.48}\text{Sr}_{0.52}\text{MnO}_3$ films

Liang, S. ; Sun, J. R.; Chen, Yunzhong; Shen, B. G.

Published in:
Journal of Applied Physics

Link to article, DOI:
[10.1063/1.3657845](https://doi.org/10.1063/1.3657845)

Publication date:
2011

Document Version
Publisher's PDF, also known as Version of record

[Link back to DTU Orbit](#)

Citation (APA):
Liang, S., Sun, J. R., Chen, Y., & Shen, B. G. (2011). Anisotropic transport behavior of orbital-ordered $\text{Nd}_{0.48}\text{Sr}_{0.52}\text{MnO}_3$ films. *Journal of Applied Physics*, 110, Article 096103. <https://doi.org/10.1063/1.3657845>

General rights

Copyright and moral rights for the publications made accessible in the public portal are retained by the authors and/or other copyright owners and it is a condition of accessing publications that users recognise and abide by the legal requirements associated with these rights.

- Users may download and print one copy of any publication from the public portal for the purpose of private study or research.
- You may not further distribute the material or use it for any profit-making activity or commercial gain
- You may freely distribute the URL identifying the publication in the public portal

If you believe that this document breaches copyright please contact us providing details, and we will remove access to the work immediately and investigate your claim.

Anisotropic transport behavior of orbital-ordered Nd_{0.48}Sr_{0.52}MnO₃ filmsS. Liang, J. R. Sun,^{a)} Y. Z. Chen, and B. G. Shen*Institute of Physics and Beijing National Laboratory for Condensed Matter Physics,
Chinese Academy of Sciences, Beijing 100190, People's Republic of China*

(Received 4 August 2011; accepted 29 September 2011; published online 3 November 2011)

Anisotropic magnetoresistance (AMR) and Hall effect have been studied for the (110)-oriented Nd_{0.48}Sr_{0.52}MnO₃ film. The most remarkable results are the significant enhancement of the AMR accompanying the orbital ordering and the appearance of four-fold symmetry of the AMR along the [1-10] direction. Analysis of the Hall data indicates the absence of any visible increase in spin-orbit coupling corresponding to the AMR growth. This suggests a different mechanism for the AMR of Nd_{0.48}Sr_{0.52}MnO₃ from that of the conventional ferromagnetic metals/alloys. © 2011 American Institute of Physics. [doi:10.1063/1.3657845]

Anisotropic magnetoresistance (AMR) is one of the most typical features of the manganite.¹⁻⁶ It behaves differently from that of the conventional ferromagnetic (FM) metals/alloys, exhibiting a sharp peak slightly below the Curie temperature (Refs. 1, 3, and 4) and a phase shift of $\pi/2$ when the manganite undergoes an insulator-metal transition.^{4,6}

A possible origin for the AMR is the spin-orbit coupling that leads to asymmetric scattering of the charge carrier with different spin orientation.⁴ However, it is believed that the orbital tilting, which may affect the Mn 3d-O 2p overlap, a the spin aligning along magnetic field could be an alternative source for the AMR.¹ There are also explanations in terms of Lorentz force-induced conductivity reduction in electronic phase-separated films (Ref. 7) and orbital ordering produced anomaly in spin-orbit interaction.⁶ Although the mechanism for the AMR is still under strong debate, spin-orbit coupling seems to be a key factor for the understanding of the unusual AMR in the manganites.

In addition to the AMR, the abnormal Hall effect provides an alternative access to the spin-orbit coupling. As theoretically predicted,⁸ for the electronic transport dominated by polaronic hopping, the anomalous Hall resistivity (AHR) will grow in proportional to the spin-orbit interaction and in reversely proportional to $n\cos^4(\Theta/2)$, where n is the carrier density and Θ is the average angle between adjacent magnetic moments. In the past decade, the Hall effect of the manganite has been intensively studied. However, less special attention has been paid to spin-orbit coupling.

A primary motivation of the present work is, via a combined study of the AMR and AHR, to get a deep understanding of the coupling between different degrees of freedom in the manganite. Nd_{0.48}Sr_{0.52}MnO₃ (NSMO) is a suitable sample for this purpose because of its distinctive features.⁹

The NSMO films were grown on (110)-oriented SrTiO₃ substrates by the pulsed laser ablation technique. The temperature of the substrate was kept at 700 °C and the oxygen pressure at 60 Pa during the deposition. The thickness of the film is \sim 180 nm, controlled by deposition time. Anisotropic transport and Hall resistance were measured by a physical

property measurement system (PPMS-14h). A bridge-shaped sample (0.1 mm in width and 0.4 mm in length) with four terminals and a Hall bar-shaped sample (0.2 mm in width and 3 mm in length) were used for corresponding measurements.

Figure 1 shows the temperature dependent resistivity (ρ) measured under different magnetic fields. Resistive anomalies corresponding to magnetic transitions can be identified in the ρ - T relations. The declining of the ρ - T curve upon cooling is caused by the FM transition, while the resistivity upturn beginning at T_N stems from the AFM transition. The magnitude of $\Delta\rho = \rho(0) - \rho(T_N)$ is much lower than that expected for a CE-AFM transition, and the ρ - T dependence is somewhat similar to that in the A-AFM single crystal of Nd_{0.45}Sr_{0.55}MnO₃, measured along the c -direction. These features are observed in both the [001] and [1-10] directions. Inset in Fig. 1 shows the magnetizations as a function of temperature. It clearly demonstrates the FM at $T_C \sim 260$ K and the AFM transitions at $T_N \sim 203$ K. These results suggest the occurrence of an orbital ordered AFM transition below T_N .

As expected, magnetic field strongly affects the magnetic transition, and the T_C varies from ~ 236 K to ~ 300 K and T_N from ~ 200 K to ~ 126 K for the field ascending from 0 to 10 T. Correspondingly, the resistivity is depressed significantly. However, the insulator-like behavior still holds at low temperatures under a field as high as 10 T.

The AMR in both the [001] and [1-10] directions was measured under the fields between 5 T and 10 T in the temperature interval from 40 K to 230 K. The angle θ between magnetic field and current was tuned from 0° to 360°. θ is set to 0° when the magnetic field is parallel to the current. The field direction is kept in the film plane. In Fig. 2, we show the angular dependent resistivity defined as $\Gamma(\theta) = [\rho(\theta) - \rho(0)]/\rho(0)$. In the [001] direction, $\Gamma(\theta)$ displays a two-fold symmetry. However, a four-fold component emerges in $\Gamma^{[1-10]}(\theta)$ below 140 K and develops with the decrease of temperature. It is a feature strongly dependent on magnetic field, weakening with the increase of H . The maximal AMR is $\sim 8\%$, obtained under a field of 10 T at the temperature of 40 K.

The isothermal magnetization was measured as a function of magnetic field at three typical temperatures 60 K,

^{a)}Author to whom correspondence should be addressed. Electronic mail: jrsun@g203.iphy.ac.c.

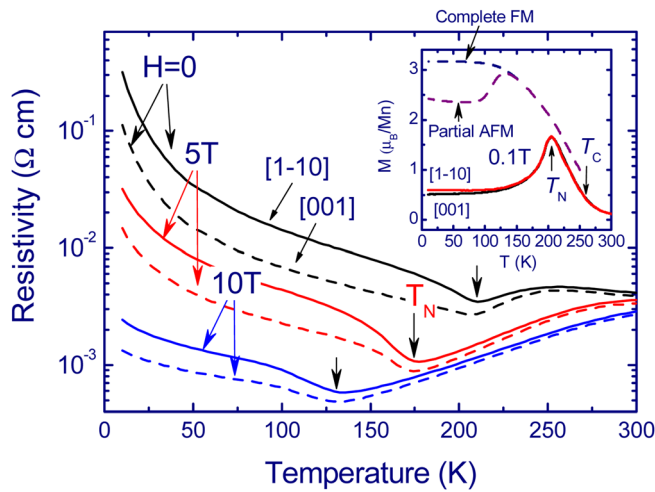


FIG. 1 (Color online) Temperature dependence of the resistivity measured along the [1-10] and [001] directions. Inset plot is the temperature-dependent magnetizations measured under a field of 0.1 T. Dashed lines are expected magnetizations after a complete (complete FM) or a partial depression (partial FM) of the AFM state.

140 K, and 170 K, and no significant differences are observed in both the [001] and [1-10] directions (not shown). It means that the AMR is an intrinsic effect.

The $\Gamma(\theta)$ relations were fitted to the following equations: $\Gamma^{[001]}(\theta) = A_0 + A_u \cos 2\theta$ and $\Gamma^{[1-10]}(\theta) = A_0 + A_u \cos 2\theta + A_c \cos 4\theta$. The results of the curve fitting are also presented in Figs. 2(a) and 2(b) (solid lines), adopting the parameters shown in Figs. 2(c) and 2(d). It is obvious that the above equations provide a satisfactory description for the experiment data. The dependence of the fitting parameters on temperature and magnetic field reveals the quantitative features of the AMR. As shown in Figs. 2(c) and 2(d), outside the transition region $A_u^{[001]}$ exhibits a linear yet slow increase with the decrease of temperature with a nearly constant $A_u^{[001]}-T$ slope of ~ 0.007 , and a sudden growth during the AFM ordering. In contrast, the $A_u^{[1-10]}-T$ relation is much more complex. The $A_u^{[1-10]}-T$ slope first inclines then declines, forming a broad maximum near T_N . Fascinatingly, it is accompanying the $A_u^{[1-10]}-T$ descending the four-fold term $A_c^{[1-10]}$ emerges and develops. In other words, $A_c^{[1-10]}$ grows at the expense of $A_u^{[1-10]}$. The $\cos 4\theta$ term was also observed before in the $\text{La}_{0.7}\text{Ca}_{0.3}\text{MnO}_3$ film when magnetic field rotated around the [001] axis, and it is likely a reflection of the cubically symmetric lattice.¹ In the present experiment, the normal direction of the film plane is [1-10], which is a two-fold lattice axis. As shown in Fig. 2(d), the four-fold feature of the AMR enhances upon cooling whereas it weakens with the increase of magnetic field, suggesting a close relation to the orbital ordering.

Sources for the magnetoresistance anisotropy fall into four categories: path-length effects, Fermi surface effects, anisotropic scattering due to the spin-orbit interaction, and orbital tilting while electron spin aligns along magnetic field. As well documented, the former two factors cannot cause the phenomena observed here. As for the spin-orbit coupling, it has been an origin for the AMR in conventional ferromagnetic metals/alloys. It affects the AMR in the form: $\text{AMR} \propto$

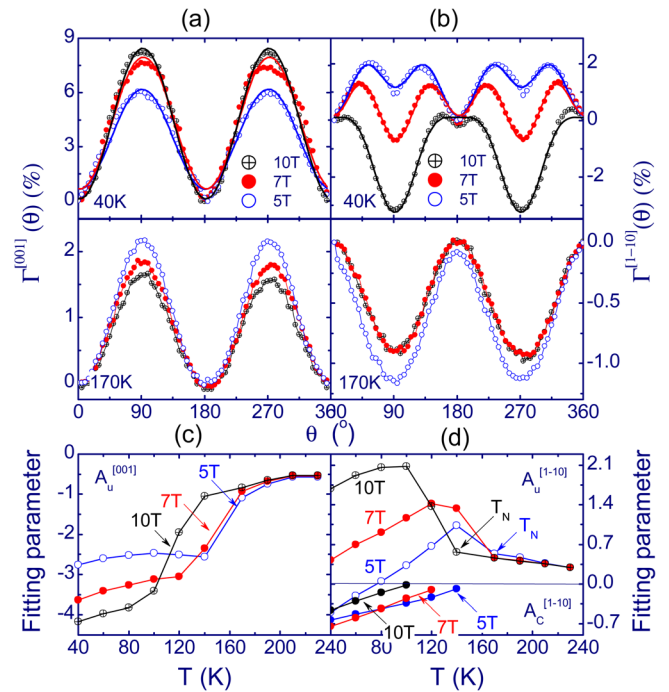


FIG. 2 (Color online) Angular dependence of the magnetoresistance measured under different magnetic fields. Data shown in (a) and (b) are obtained with the current applied in the [001] and [1-10] direction, respectively. Results of curve fitting are presented as solid curves in two top panels. The corresponding fitting parameters are shown in (c) and (d).

$m^2 \lambda_{\text{SO}}$,¹⁰ where m is the normalized magnetization and λ_{SO} is a parameter describing the spin-orbit coupling. Whether the abnormal AMR is due to an enhancement of the spin-orbit coupling is an issue deserves further investigations. For this purpose, the Hall resistivity ρ_{xy} of the NSMO films was studied.

As expected, the Hall resistivity ρ_{xy} , measured along the [1-10] direction, undergoes first a sudden drop, then a linear growth with the increase of magnetic field (not shown). The former is called anomalous Hall resistivity and the latter is the ordinary one. A simple description has been given to the Hall resistivity: $\rho_{xy} = R_A \mu_0 M + R_H \mu_0 H$, where R_A and R_H are the anomalous and ordinary Hall coefficients, respectively, μ_0 the vacuum permeability, and M the magnetization. The slope of the $\rho_{xy} - \mu_0 H$ curves is positive, which indicates the hole-like character of the charge carriers. In the temperature region between 200 K and 260 K, where the NSMO film is in the metallic FM state, the ordinary Hall resistivity changes with magnetic field linearly. The carrier density can be deduced from the $\rho_{xy} - \mu_0 H$ curves. We estimate the carrier density $n = e^{-1} d\rho_{xy} / d\mu_0 H$ based on the $\rho_{xy} - \mu_0 H$ curves near 10 T. As shown in Fig. 3, the carrier density exhibits first a gradual growth when cooled from ~ 230 K to ~ 120 K, then an obvious decrease for further cooling. The anomalous Hall resistivity ρ_A can be obtained by extrapolating the high field part ($H > 6$ T) of the $\rho_{xy} - \mu_0 H$ curve to the limit of $H \rightarrow 0$. The results thus obtained are presented in Fig. 3 (red symbols). It shows that ρ_A is low at low temperatures, and exhibits first a slow then a rapid growth upon warming.

Based on the Hall resistivity, an expression for λ_{SO} can be derived: $\lambda_{\text{SO}}(\text{AHR}) \propto \rho_A n \cos^4(\Theta/2) = \rho_A n (1 + m^2)^2$ here the

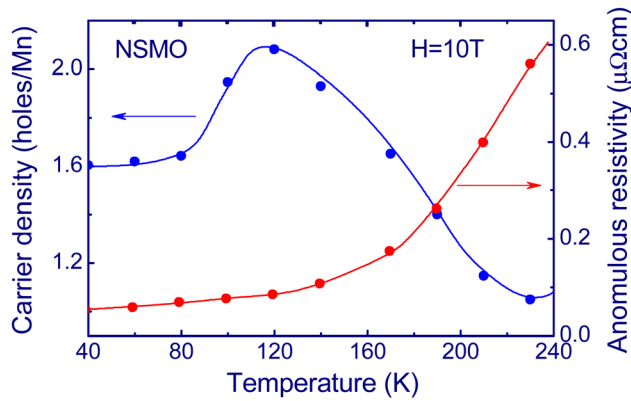


FIG. 3 (Color online) Temperature dependence of carrier density obtained under the field of 10 T (left) and the anomalous Hall resistivity (right).

equality of $\cos^4(\Theta/2) = (1 + m^2)/4$ has been utilized. Figure 4 presents the temperature-dependent spin-orbit coupling constant calculated by this formula, where the schematic M - T relation (dashed lines) in the inset of Fig. 1 has been adopted for the calculation. The λ_{SO} calculated by $\lambda_{SO}^2(\text{AMR}) \propto \Gamma^{[1-10]}/m^2$ is also presented for comparison. Fascinatingly, $\lambda_{SO}(\text{AHR})$ displays a smooth decrease as temperature reduces from 230 K to 40 K, with a visible downward shift beginning at ~ 120 K. This result means a weakening of the spin-orbit coupling upon the AFM transition. It is completely different from the behavior deduced from the AMR data, which shows a sudden jump near ~ 120 K. It is therefore possible that the AMR mechanism for the manganites is different from that for the conventional metals/alloys. The magnetization of the NSMO film cannot be accurately determined under a high applied field. Although the detailed shape of the M - T curve may affect the λ_{SO}^2 - T relation, it cannot convert the jump to the drop of $\lambda_{SO}(\text{AHR})$.

As well documented, spins have a preferred direction with respect to the orbital orientation for the manganite, and the orbital and spin ordering can be tuned by lattice strains.¹¹ This actually implies the presence of some kind spin-orbit coupling. This form of spin-orbit coupling may affect the AMR in a manner different from that in the metals/alloys. Although the detailed mechanism for the AMR cannot be definitely determined, the present work seems to support the field-induced orbital-tilting proposed by O'Donnell *et al.* As well documented, the transport in the manganite realizes via the overlapped Mn 3d-O 2p orbitals. Magnetic field may affect this process by modifying orbital orientation, thus the conduction band via aligning spins. This effect could be strongly anisotropic in the orbital-ordered AFM state due to the presence of preferred orbital orientation, which explains the significant AMR below the AFM transition.

The AMR of the charge-and-orbital-ordered SCMO film displays a crossover from positive to negative when the film

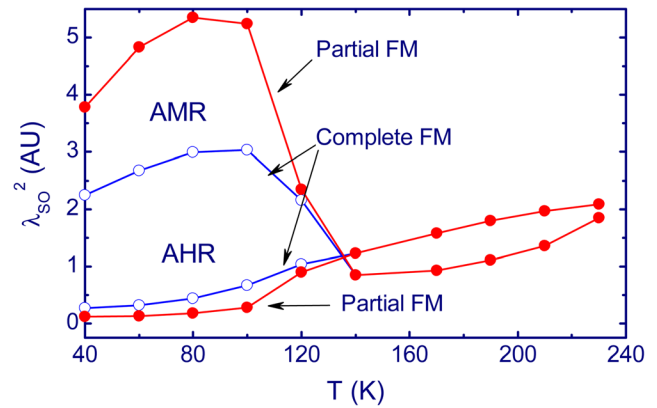


FIG. 4 (Color online) Spin-orbit coupling parameters determined by anomalous Hall resistivity (marked by AHR) and anisotropic magnetoresistance (marked by AMR), respectively. Complete FM and partial FM denote the results calculated from the corresponding M - T curves in the inset plot of Fig. 1.

transits from insulating to metallic. This feature is not observed in the present sample. However, a careful investigation of the fitting parameter in Fig. 2(d) reveals a reduction of $A_u^{[001]}$ upon cooling under the field of 5 T: $A_u^{[001]}$ is negative in insulating state and positive in metallic state. Therefore, the two-fold parameter of the NSMO film shares the same feature with that of SCMO. The four-fold symmetry is interesting. It does not hold for the lattice with the axis of $[1-10]$. This phenomenon may stem from the special symmetry of the AFM and orbital orderings of NSMO.

This work has been supported by the National Basic Research of China, the National Natural Science Foundation of China, the Knowledge Innovation Project of the Chinese Academy of Science, the Beijing Municipal Nature Science Foundation.

¹J. O'Donnell, J. N. Eckstein, and M. S. Rzchowski, *Appl. Phys. Lett.* **76**, 218 (2000).

²Q. Li, H. S. Wang, Y. F. Hu, and E. Wertz, *J. Appl. Phys.* **87**, 5573 (2000).

³M. Bibes, V. Laukhin, S. Valencia, B. Martínez, and J. Fontcuberta, *J. Phys.: Condens. Matter* **17**, 2733 (2005).

⁴I. C. Infante, V. Laukhin, F. Sánchez, and J. Fontcuberta, *J. Appl. Phys.* **99**, 08C502 (2006).

⁵M. Egilmez, M. Saber, A. Mansour, R. C. Ma, K. H. Chow, and J. Jung, *Appl. Phys. Lett.* **93**, 182505 (2008).

⁶Y. Z. Chen, J. R. Sun, T. Y. Zhao, J. Wang, Z. H. Wang, B. G. Shen, and N. Pryds, *Appl. Phys. Lett.* **95**, 132506 (2009).

⁷M. Egilmez, R. Patterson, K. H. Chow, and J. Jung, *Appl. Phys. Lett.* **90**, 232506 (2007).

⁸Y. Lyanda-Geller, S. H. Chun, M. B. Salamon, P. M. Goldbart, and P. D. Han, Y. Tomioka, A. Asamitsu, and Y. Tokura, *Phys. Rev. B* **63**, 184426 (2001).

⁹R. Kajimoto, H. Yoshizawa, H. Kawano, and Y. Tokura, *Phys. Rev. B* **60**, 9506 (1999).

¹⁰I. A. Campbell and A. Fert, in *Ferromagnetic Materials*, edited by E. P. Wohlfarth (North-Holland, Amsterdam, 1982), Vol. 3, p. 747; I. A. Campbell, A. Fert, and O. Jaoul, *J. Phys. C*, S95 (1970).

¹¹Y. Tokura and N. Nagaosa, *Science* **288**, 462 (2002); Y. Okimoto, Y. Konishi, M. Izumi, T. Manako, M. Kawasaki, and Y. Tokura, *J. Phys. Soc. Jpn.* **71**, 613 (2002).